ACS OMEGA

http://pubs.acs.org/journal/acsodf

Article

Angular-Independent Structural Colors of Clay Dispersions

Nobuyoshi Miyamoto* and Shinya Yamamoto

Cite This: *ACS Omega* 2022, 7, 6070−6074

Read Online

ACCESS | Metrics & More | Article Recommendations | Supporting Information

ABSTRACT: Clay mineral nanosheet colloids were found to show angular-independent structural colors after desalting. Naked-eye observation and UV−visible reflectance spectra showed that the color is tuned by varying the average nanosheet size and nanosheet concentration. The low angular-dependence of the structural color was also clarified by these observations, which is the first case for a nanosheet system. The present system is expected as an environmentally benign and low-cost structural color material for various applications.

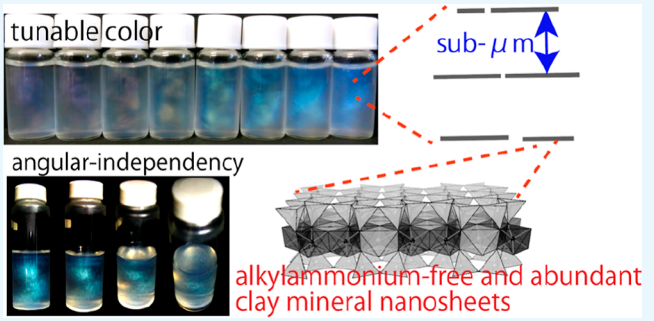

INTRODUCTION

For several thousands of years, layered clay minerals have been utilized as important functional materials for many applications. Nowadays, utilizing the inherent two-dimensional nanostructure of the clay minerals, various clay-based nanomaterials are fabricated by hybridizing with functional molecules and polymers in organized manners in the nanometer scale.[1] Many kinds of layered materials with various functionalities and chemical compositions have been developed and their applications for various nanomaterials have been reported.[2−4] Among those layered materials, clay minerals are most important for practical industrial applications because they are composed of abundant elements such as Si, Al, and O and are low cost, stably supplied, harmless, biocompatible, and environmentally friendly. In addition, the recent rediscovery of clay colloids as lyotropic liquid crystals (LCs)[5−8] opened new applications as anisotropic functional biopolymer/inorganic composites,[9] gel actuators,[10,11] and polymer composites with excellent gas-barrier[12] and mechanical[13] properties. Macroscopic ordering of the clay LC phase by external field[10,14−16] opens further sophisticated anisotropic materials.

Meanwhile, structural color materials, of which color occurs due to interference of light, are recently extensively investigated for potential applications as sensors and weather-resistant coloring materials.[17−22] However, the lowering of unfavorable angular-dependence, improvement of color gamut, better durability, and simple and low-cost synthesis are remaining as challenging issues for practical applications. Although a part of these problems has been solved by recent studies,[17] further improvements are desired. To break these technical barriers, the development of a brand new type of structural color materials are expected; however, most of the structural color materials reported so far are limited to cholesteric LCs,[23] surfactant solutions,[24] and spherical colloids[25] of polymers or oxides.

In this situation, a new-type structural color material of LC nanosheets is emerging. Gabriel et al. first reported the antimony phosphate nanosheet with structural color,[26] followed by several researchers' reports on zirconium phosphate,[27] titanate,[28] hexaniobate,[29] graphene oxide,[30] and layered perovskites.[31] However, it is still problematic that high-cost rare elements such as antimony and zirconium are not suitable for industrial applications. Harmful and smelly exfoliation agent such as alkylammonium to stabilize the nanosheet dispersion is also problematic. To synthesize most of these materials, calcination at high temperature is required, which is energy-wasting.

Herein, we demonstrate a nanosheet-based angular-independent structural color material for the first time. The material is composed of environmentally benign, low-cost, alkylammonium-free clay mineral nanosheets, and the color is tuned over a full range of visible light independently by nanosheet lateral size and nanosheet concentration.

RESULTS AND DISCUSSION

Various structural colors were observed in the nanosheet colloid (D_{ave} = 1.8 μm) under white illumination, depending on the nanosheet concentration c, as shown in Figure 1A. The color is not very strong but is clearly visible when a black background is placed behind the sample. With c = 1.9 wt %,

Received: November 15, 2021
Accepted: January 27, 2022
Published: February 11, 2022

https://doi.org/10.1021/acsomega.1c06448
ACS Omega 2022, 7, 6070−6074

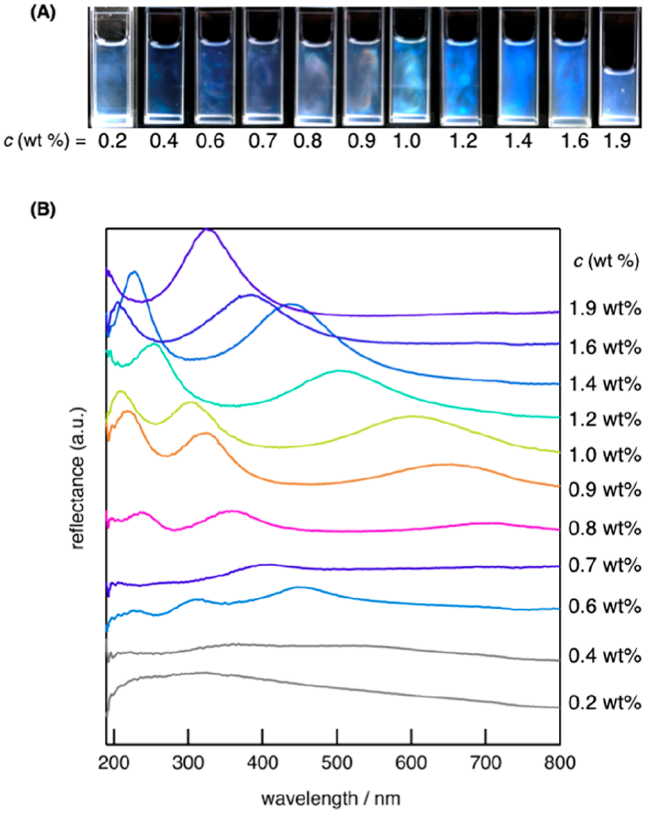

Figure 1. (A) Photographs and (B) the UV−visible reflectance spectra of the nanosheet colloids (D_{ave} = 1.8 μm) with various nanosheet concentrations c measured at α = 10°.

pale purple color was observed. The color changed to blue (1.6 and 1.4 wt %), green (1.2 wt %), yellow (1.0 wt %), orange (0.9 wt %), and red (0.8 wt %) as the nanosheet concentration decreased. By further decreasing the concentration, the purple and blue structural colors were again observed at 0.7 and 0.6 wt %. Below 0.6 wt %, the colloid showed no structural color, while it was slightly turbid due to scattering from the nanosheets. While the color of an as-prepared sample changed after days and weeks probably due to the absorption of carbon dioxide that causes slight changes in ionic strength, we confirmed that the color was recovered by washing by centrifugation again. Afterward, the structural colored colloidal samples were very stable for years without the formation of agglomerates because of the strong repulsion between the nanosheets that arises from the negative charge of the nanosheets as explained by the DLVO theory. The coloration and its tunability by c are mostly reproducible as confirmed by the observation of another batch of the samples (Figure S1).

To investigate the structural colors in detail, the UV−vis reflection spectra were recorded (Figure 1B). At c = 1.9 wt %, the maximum reflection wavelength λ_{max} was 327 nm. The reflection peak shifted to longer wavelengths and became broader with the decrease of c. The peak accompanied the second, third, or forth order peaks at $\lambda_{max}/2$, $\lambda_{max}/3$, and $\lambda_{max}/4$. The λ_{max} corresponds to the observed colors. From the spectrum measurement, we confirmed that the blue structural color observed at c = 0.6 vol % is due to the secondary peak at 430 nm.

The structural color of the nanosheet colloid was also controllable by D_{ave}. We conducted visual observation and reflection spectroscopy (Figure 2) for a single batch sample (c = 1.0 wt %, D_{ave} = 1.8 μm) in the process of ultrasonication for 22, 40, and 60 min. After ultrasonication, D_{ave} was reduced to 0.98, 0.16, and 0.14 μm, respectively (Figure S2). The structural color changed from yellow (0 min) to green (22 min) and light blue (40 min) and finally to blue (60 min) as the sample was ultrasonicated. The half width of the reflection peak decreased with the decrease in D_{ave}, indicating that the structural regularity is increasing. The control sample that was just stood without ultrasonication showed no color change. This phenomenon is explained by considering that D_{ave} significantly affects the isotropic/nematic phase transition[32] and resulting superstructures.[34] Although the effects of D_{ave} on the structural colors of nanosheet colloid have rarely been reported,[30] this will be generalized to various nanosheet systems.

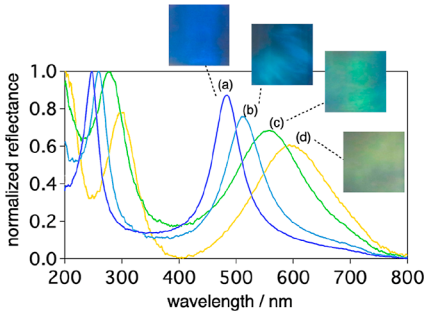

Figure 2. Photographs and UV−vis spectra of the nanosheet colloid with the D_{ave} of (a) 0.14, (b) 0.16 (c) 0.98, and (d) 1.8 μm. The spectra were recorded at α = 10°.

It is notable that the structural color of the present system showed no angular dependence as visually shown in Figure 3.

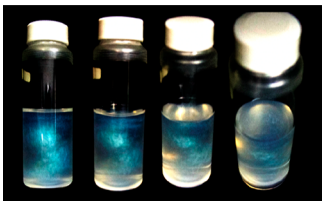

Figure 3. Photographs of the clay colloid (0.8 wt %, batch C) with green structural color viewed from different angles.

Figure 4A shows the dependence of the reflectance spectrum of the sample (c = 1.0 wt %, D_{ave} = 1.8 μm) on the observing angle α. Although the reflectance varies with α, λ_{max} is almost constant. The independence of λ_{max} on α was confirmed for all the samples with various nanosheet concentrations (Figure 4B).

As a possible explanation for the angular-independent structural color of the present system, we consider that the color arises from randomly oriented 10−100 μm scale lamellar LC domains[6] in which nanosheets are stacked with sub-micrometer periodicity. According to Bragg-Snell's law, the wavelength λ_{max} of the light reflected by a crystal is expressed as

$$\lambda_{max} = (2d/m)(n^2 - \sin^2\theta)^{1/2} \quad (1)$$

where d is the periodic distance of the crystal, θ is the incident angle, n is the average refractive index of the crystal, and m is the diffraction order. Here, the incident angle θ is equal to the angle between the normal of the lamellar plains and the

https://doi.org/10.1021/acsomega.1c06448
ACS Omega 2022, 7, 6070−6074

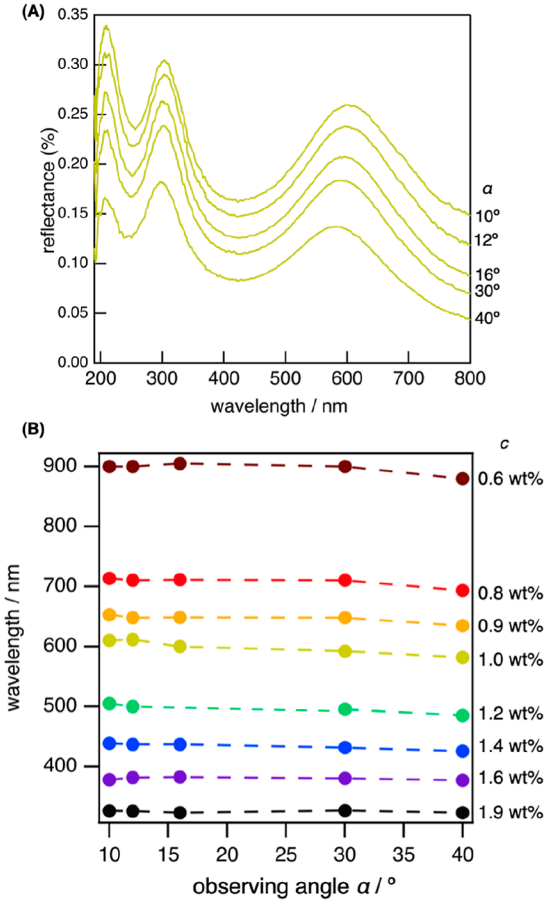

Figure 4. (A) Angular dependence of the UV−vis reflectance spectrum of the clay nanosheet colloid (D_{ave} = 1.8 nm, c = 1.0 wt %). (B) Dependence of λ_{max} on the observing angle α of the nanosheet colloids (D_{ave} = 1.8 nm) with varied nanosheet concentrations c.

observing direction. The dependence of λ_{max} on the nanosheet concentration c (shown in Figure 1) is explained based on this equation because d decreases with c, according to a general swelling law. Because LC domains have a random orientation, we expect a certain averaged λ_{max}, considering that the incident light is stronger for smaller θ because of the black background, as schematically shown in Scheme 1. Meanwhile, in the small-angle X-ray scattering (SAXS) measurement (Figure S3a), a structural colored clay colloid sample showed the peaks due to the periodic distance $d \sim 170$ nm, while λ_{max} was around 500 nm in the UV−vis spectra (Figure S3b). This experimental result is mostly in accordance with the calculation. With d = 170 nm, n = 1.33 (water), and m = 1, λ_{max} is calculated as 452 nm for $\theta = 0°$.

Scheme 1. Schematic Representation of the Present Study: Angular-Independent Structural Color due to Randomly Oriented Lamellar Domains of Clay Nanosheets Dispersed in Water

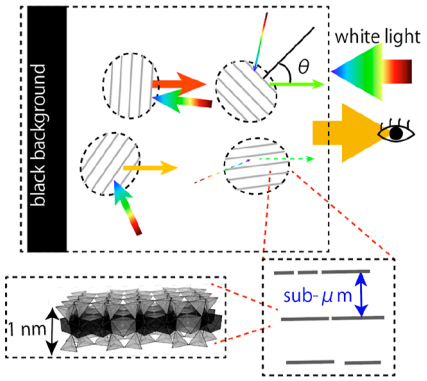

To further discuss the mechanism mentioned above, we conducted a rough numerical calculation of a theoretical reflection spectrum. We calculate the theoretical reflectance spectrum of randomly oriented lamellar domains dispersed in water as follows. We consider a lamellar domain composed of N layers, where the refractive index of the i_{th} layer is n_i, is dispersed in a solvent with the refractive index n_0. Based on the multilayer interference model, the reflectance of the incident s-wave light $S(\theta, \lambda)$ is calculated as $|s_N(\theta, \lambda)|^2$ that is obtained from the following function series

$$t_j(\theta) = \frac{n_{j+1}c_{j+1}(\theta) - n_j c_j(\theta)}{n_{j+1}c_{j+1}(\theta) + n_j c_j(\theta)}$$

$$s_0(\theta, \lambda) = t_0(\theta)$$

$$s_j(\theta, \lambda) = \frac{t_j(\theta) + s_{j-1}(\theta, \lambda)\exp(i\cdot\Delta_j(\theta, \lambda))}{1 + s_{j-1}(\theta, \lambda)t_j(\theta)\exp(i\cdot\Delta_j(\theta, \lambda))}$$

$$\text{with } j = 1,2, \ldots N$$

where

$$c_j(\theta) = \sqrt{1 - \left(\frac{n_0}{n_j}\sin\theta\right)^2}$$

$$\Delta_j(\theta, \lambda) = \frac{4\pi n_j d_j c_{j+1}}{\lambda}$$

The reflectance spectrum of the incident p-wave light $P(\alpha, \lambda)$ is similarly calculated with

$$q_i(\theta) = \frac{n_{j+1}c_j(\theta) - n_j c_{j+1}(\theta)}{n_{j+1}c_j(\theta) + n_j c_{j+1}(\theta)}$$

$$p_0(\theta, \lambda) = q_0(\theta)$$

$$p_j(\theta, \lambda) = \frac{q_j(\theta) + p_{j-1}(\theta, \lambda)\exp(i\bullet\Delta_j(\theta, \lambda))}{1 + p_{j-1}(\theta, \lambda)q_j(\theta)\exp(i\bullet\Delta_j(\theta, \lambda))}$$

$$\text{with } j = 1,2, \ldots N$$

Supposing that the incident light is nonpolarized light, the reflectance $R(\theta, \lambda)$ is obtained as the average of the results for s- and p-waves.

$$R(\theta, \lambda) = \frac{P(\theta, \lambda) + S(\theta, \lambda)}{2}$$

Considering the uniform random distribution of θ and supposing that the incident light intensity is proportional to $\theta/(\pi/4)$ because the background is black, the reflectance spectrum $R_{total}(\lambda)$ is calculated as the integral over the angle θ as

https://doi.org/10.1021/acsomega.1c06448
ACS Omega 2022, 7, 6070−6074

$$R_{\text{total}}(\lambda) = \int_0^{\pi/4} R(\theta, \lambda)\frac{\theta}{\pi/4}\sin\theta \mathrm{d}\theta$$

To consider LC domains composed of water layer (169 nm thick and n = 1.3) and nanosheet layer (1 nm and n = 1.6), we set N = 19, n_j = {1.6, 1.3, 1.6, ...1.3, 1.6} and d_j = {1, 169, ..., 1, 169, 1}. As the result (Figure 5), the calculated spectra are dependent on the orientation angle θ of the LC domains (dotted lines), while the averaged spectrum (bold line) shows a peak at λ_{max} = 420 nm, which is not far from the experimental result (Figure S3). We plan more precise calculations and consideration of other proposed models[17] in future works to further investigate the mechanism for the angular-independent structural color in the present nanosheet based system.

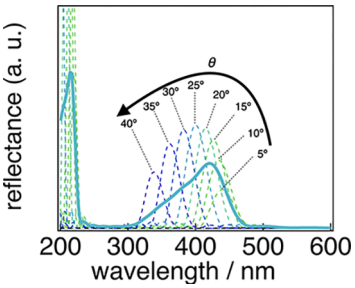

Figure 5. Reflectance spectra that were numerically calculated based on the multilayer interference model. The dotted lines are the spectra of lamellar domains with varied θ, the angle between the observing direction and the normal of the lamellar plain of liquid crystalline domains. The bold line is the spectra averaged over θ.

CONCLUSIONS

A nanosheet colloid was for the first time demonstrated as an angular-independent structural color material. The color was tuned by nanosheet lateral size as well as by nanosheet concentration. Because the present system is composed of environmentally benign clay mineral, low-cost industrial applications such as pigment, smart windows, and sensors are expected. In view of these applications, further fundamental research studies are underway to improve color brightness considering the refractive index, layer thickness, and the structural regularity as well as to immobilize the structural colloid as a solid material.

EXPERIMENTAL SECTION

Materials and Sample Preparations. The layered clay mineral fluorohectorite [FHT; $Na_{0.46}(Mg_{2.60}Li_{0.46})Si_4O_{10}F_{2.00}$] was supplied from Topy Industries Ltd. and purified before use as described in the literature.[6] Purified FHT colloid (8.1 wt %) contained the single-layer nanosheets with the thickness of 1 nm as observed by atomic force microscopy (AFM) (Figure S4). The average lateral size D_{ave} was determined as 1.8 μm by dynamic light scattering (DLS) (Figure S5). The nanosheet colloid was ultrasonicated with a Fine FU-21H ultrasonic bath for up to 60 min to obtain the samples with reduced D_{ave}. As reported in the literature,[6,32,33] the lateral size of the nanosheets is reduced by ultrasonication. The as-prepared colorless colloid was desalted by centrifugation or dialysis to obtain structural colored samples. In addition to the main sample batch A mentioned above, we also prepared, by the same procedure, batches B and C to check the reproducibility and to conduct additional experiments shown in Figures 3, S1, and S3.

Characterizations. The DLS measurements were performed on Ohtsuka Electronics DLS-8000. The AFM images were obtained with a Nanocute (SII Nano Technology Inc). Angular-dependent reflectance spectra were recorded on the spectrophotometer V650 (JASCO) equipped with the absolute reflectance measurement unit ARSV732 (JASCO). The spectrophotometer was calibrated before the sample measurement. By covering the entrance of the integrating sphere with a black paper, dark measurement was done. After that, the water in a cell was measured as the baseline with the observing angle α = 180° (Scheme S3a) and samples were measured with α = 10−40° (Scheme S3b). SAXS was measured on a Rigaku NANOPIX with CuKα radiation.

ASSOCIATED CONTENT

Supporting Information

The Supporting Information is available free of charge at https://pubs.acs.org/doi/10.1021/acsomega.1c06448.

Photograph and UV−vis reflectance spectra; particle size distributions of the nanosheets measured by DLS; SAXS and the UV−vis reflectance spectra; AFM image of the FHT nanosheets; and setup for angular-dependent UV−vis reflectance spectra (PDF)

AUTHOR INFORMATION

Corresponding Author

Nobuyoshi Miyamoto − *Department of Life, Environment, and Applied Chemistry, Fukuoka Institute of Technology, Fukuoka 811-0295, Japan;* orcid.org/0000-0001-5200-2540; Email: miyamoto@fit.ac.jp

Author

Shinya Yamamoto − *Department of Life, Environment, and Applied Chemistry, Fukuoka Institute of Technology, Fukuoka 811-0295, Japan*

Complete contact information is available at: https://pubs.acs.org/10.1021/acsomega.1c06448

Author Contributions

N.M. designed the research and wrote the manuscript. S.Y. conducted the experiments and data analyses.

Notes

The authors declare no competing financial interest.

ACKNOWLEDGMENTS

This research work was partly supported by "Innovation inspired by Nature" Research Support Program of Sekisui Chemical Co. Ltd; Program for Creating STart-ups from Advanced Research and Technology of Japan Science and Technology Agency (JST-SCORE); and Electronics Research Laboratory of Fukuoka Institute of Technology.

REFERENCES

(1) Nakato, T.; Kawamata, J.; Takagi, S. *Inorganic Nanosheets and Nanosheet-Based Materials*; Springer Japan: Tokyo, 2017.

(2) Geng, F.; Ma, R.; Ebina, Y.; Yamauchi, Y.; Miyamoto, N.; Sasaki, T. Gigantic Swelling of Inorganic Layered Materials: A Bridge to Molecularly Thin Two-Dimensional Nanosheets. *J. Am. Chem. Soc.* **2014**, *136*, 5491−5500.

(3) Geng, F.; Ma, R.; Nakamura, A.; Akatsuka, K.; Ebina, Y.; Yamauchi, Y.; Miyamoto, N.; Tateyama, Y.; Sasaki, T. Unusually stable ~100-fold reversible and instantaneous swelling of inorganic layered materials. *Nat. Commun.* **2013**, *4*, 1632.
(4) Bastakoti, B. P.; Li, Y.; Imura, M.; Miyamoto, N.; Nakato, T.; Sasaki, T.; Yamauchi, Y. Polymeric micelle assembly with inorganic nanosheets for construction of mesoporous architectures with crystallized walls. *Angew. Chem., Int. Ed.* **2015**, *54*, 4222−4225.
(5) Michot, L. J.; Bihannic, I.; Maddi, S.; Funari, S. S.; Baravian, C.; Levitz, P.; Davidson, P. Liquid-crystalline aqueous clay suspensions. *Proc. Natl. Acad. Sci. U.S.A.* **2006**, *103*, 16101−16104.
(6) Miyamoto, N.; Iijima, H.; Ohkubo, H.; Yamauchi, Y. Liquid crystal phases in the aqueous colloids of size-controlled fluorinated layered clay mineral nanosheets. *Chem. Commun.* **2010**, *46*, 4166−4168.
(7) Ringdal, N. I.; Fonseca, D. M.; Hansen, E. L.; Hemmen, H.; Fossum, J. O. Nematic textures in colloidal dispersions of Na-fluorohectorite synthetic clay. *Phys. Rev. E: Stat., Nonlinear, Soft Matter Phys.* **2010**, *81*, 041702.
(8) Paineau, E.; Antonova, K.; Baravian, C.; Bihannic, I.; Davidson, P.; Dozov, I.; Impéror-Clerc, M.; Levitz, P.; Madsen, A.; Meneau, F.; Michot, L. J. Liquid-Crystalline Nematic Phase in Aqueous Suspensions of a Disk-Shaped Natural Beidellite Clay. *J. Phys. Chem. B* **2009**, *113*, 15858−15869.
(9) Kato, R.; Kakugo, A.; Shikinaka, K.; Ohsedo, Y.; Kabir, A. M. R.; Miyamoto, N. Liquid Crystalline Colloidal Mixture of Nanosheets and Rods with Dynamically Variable Length. *ACS Omega* **2018**, *3*, 14869−14874.
(10) Inadomi, T.; Ikeda, S.; Okumura, Y.; Kikuchi, H.; Miyamoto, N. Photo-Induced Anomalous Deformation of Poly(N -Isopropylacrylamide) Gel Hybridized with an Inorganic Nanosheet Liquid Crystal Aligned by Electric Field. *Macromol. Rapid Commun.* **2014**, *35*, 1741−1746.
(11) Zhu, Q. L.; Dai, C. F.; Wagner, D.; Daab, M.; Hong, W.; Breu, J.; Zheng, Q.; Wu, Z. L. Distributed Electric Field Induces Orientations of Nanosheets to Prepare Hydrogels with Elaborate Ordered Structures and Programmed Deformations. *Adv. Mater.* **2020**, *32*, 2005567.
(12) Tsurko, E. S.; Feicht, P.; Nehm, F.; Ament, K.; Rosenfeldt, S.; Pietsch, I.; Roschmann, K.; Kalo, H.; Breu, J. Large Scale Self-Assembly of Smectic Nanocomposite Films by Doctor Blading versus Spray Coating: Impact of Crystal Quality on Barrier Properties. *Macromolecules* **2017**, *50*, 4344−4350.
(13) Morooka, T.; Ohsedo, Y.; Kato, R.; Miyamoto, N. Structure-regulated tough elastomers of liquid crystalline inorganic nanosheet/polyurethane nanocomposites. *Mater. Adv.* **2021**, *2*, 1035−1042.
(14) Tominaga, M.; Nagashita, T.; Kumamoto, T.; Higashi, Y.; Iwai, T.; Nakato, T.; Suzuki, Y.; Kawamata, J. Radiation Pressure Induced Hierarchical Structure of Liquid Crystalline Inorganic Nanosheets. *ACS Photonics* **2018**, *5*, 1288−1293.
(15) Miyamoto, N.; Shintate, M.; Ikeda, S.; Hoshida, Y.; Yamauchi, Y.; Motokawa, R.; Annaka, M. Liquid crystalline inorganic nanosheets for facile synthesis of polymer hydrogels with anisotropies in structure, optical property, swelling/deswelling, and ion transport/fixation. *Chem. Commun.* **2013**, *49*, 1082−1084.
(16) Dozov, I.; Paineau, E.; Davidson, P.; Antonova, K.; Baravian, C.; Bihannic, I.; Michot, L. J. Electric-Field-Induced Perfect Anti-Nematic Order in Isotropic Aqueous Suspensions of a Natural Beidellite Clay. *J. Phys. Chem. B* **2011**, *115*, 7751−7765.
(17) Takeoka, Y.; Yoshioka, S.; Takano, A.; Arai, S.; Nueangnoraj, K.; Nishihara, H.; Teshima, M.; Ohtsuka, Y.; Seki, T. Production of colored pigments with amorphous arrays of black and white colloidal particles. *Angew. Chem., Int. Ed.* **2013**, *52*, 7261−7265.
(18) Zhou, J.; Han, P.; Liu, M.; Zhou, H.; Zhang, Y.; Jiang, J.; Liu, P.; Wei, Y.; Song, Y.; Yao, X. Self-Healable Organogel Nanocomposite with Angle-Independent Structural Colors. *Angew. Chem., Int. Ed.* **2017**, *56*, 10462−10466.
(19) Li, K.; Li, T.; Zhang, T.; Li, H.; Li, A.; Li, Z.; Lai, X.; Hou, X.; Wang, Y.; Shi, L.; Li, M.; Song, Y. Facile full-color printing with a single transparent ink. *Sci. Adv.* **2021**, *7*, No. eabh1992.
(20) Li, Y.; Liu, Z.; Zhu, K.; Ai, L.; Jia, P.; Wu, N.; Yu, H.; Wang, J.; Yao, X.; Zhou, J.; Song, Y. Inkjet Printed Physically-Unclonable Structural-Color Anticounterfeiting Labels with Convenient Artificial Intelligence Authentication. *Adv. Mater. Interfaces* **2021**, *8*, 2101281.
(21) He, X.; Gu, Y.; Yu, B.; Liu, Z.; Zhu, K.; Wu, N.; Zhao, X.; Wei, Y.; Zhou, J.; Song, Y. Multi-mode structural-color anti-counterfeiting labels based on physically unclonable amorphous photonic structures with convenient artificial intelligence authentication. *J. Mater. Chem. C* **2019**, *7*, 14069−14074.
(22) Zhang, Y.; Han, P.; Zhou, H.; Wu, N.; Wei, Y.; Yao, X.; Zhou, J.; Song, Y. Highly Brilliant Noniridescent Structural Colors Enabled by Graphene Nanosheets Containing Graphene Quantum Dots. *Adv. Funct. Mater.* **2018**, *28*, 1802585.
(23) Makow, D. M.; Sanders, C. L. Additive colour properties and colour gamut of cholesteric liquid crystals. *Nature* **1978**, *276*, 48−50.
(24) Yue, Y.; Kurokawa, T.; Haque, M. A.; Nakajima, T.; Nonoyama, T.; Li, X.; Kajiwara, I.; Gong, J. P. Mechano-actuated ultrafast full-colour switching in layered photonic hydrogels. *Nat. Commun.* **2014**, *5*, 4659.
(25) Asher, S. A.; Holtz, J.; Liu, L.; Wu, Z. Self-assembly motif for creating submicron periodic materials. Polymerized crystalline colloidal arrays. *J. Am. Chem. Soc.* **1994**, *116*, 4997−4998.
(26) Gabriel, J.-C. P.; Camerel, F.; Lemaire, B. J.; Desvaux, H.; Davidson, P.; Batail, P.; Batail, P. Swollen liquid-crystalline lamellar phase based on extended solid-like sheets. *Nature* **2001**, *413*, 504−508.
(27) Wong, M.; Ishige, R.; Hoshino, T.; Hawkins, S.; Li, P.; Takahara, A.; Sue, H.-J. Solution Processable Iridescent Self-Assembled Nanoplatelets with Finely Tunable Interlayer Distances Using Charge- and Sterically Stabilizing Oligomeric Polyoxyalkyleneamine Surfactants. *Chem. Mater.* **2014**, *26*, 1528.
(28) Sano, K.; Kim, Y. S.; Ishida, Y.; Ebina, Y.; Sasaki, T.; Hikima, T.; Aida, T. Photonic water dynamically responsive to external stimuli. *Nat. Commun.* **2016**, *7*, 12559.
(29) Mouri, E.; Ogami, C.; Fukumoto, T.; Nakato, T. Development of Structural Color by Niobate Nanosheet Colloids. *Chem. Lett.* **2020**, *49*, 717−720.
(30) Li, P.; Wong, M.; Zhang, X.; Yao, H.; Ishige, R.; Takahara, A.; Miyamoto, M.; Nishimura, R.; Sue, H.-J. Tunable Lyotropic Photonic Liquid Crystal Based on Graphene Oxide. *ACS Photonics* **2014**, *1*, 79−86.
(31) Yang, W.; Yamamoto, S.; Sueyoshi, K.; Inadomi, T.; Kato, R.; Miyamoto, N. Perovskite Nanosheet Hydrogels with Mechanochromic Structural Color. *Angew. Chem., Int. Ed.* **2021**, *60*, 8466−8471.
(32) Miyamoto, N.; Nakato, T. Liquid Crystalline Nanosheet Colloids with Controlled Particle Size Obtained by Exfoliating Single Crystal of Layered Niobate K4Nb6O17. *J. Phys. Chem. B* **2004**, *108*, 6152−6159.
(33) Mellado, C.; Figueroa, T.; Baez, R.; Meléndrez, M.; Fernández, K. Effects of probe and bath ultrasonic treatments on graphene oxide structure. *Mater. Today Chem.* **2019**, *13*, 1−7.
(34) Yamaguchi, D.; Miyamoto, N.; Fujita, T.; Nakato, T.; Koizumi, S.; Ohta, N.; Yagi, N.; Hashimoto, T. Aspect Ratio Dependent Phase Transitions and Concentration Fluctuations in Aqueous Colloidal Dispersions of Charged Plate-Like Particles. *Phys. Rev. E: Stat., Nonlinear, Soft Matter Phys.* **2012**, *85*, 011403.

https://doi.org/10.1021/acsomega.1c06448
ACS Omega 2022, 7, 6070−6074